JOURNAL OF MATERIALS SCIENCE 26 (1991) 2603–2607

Effects of annealing on the damage morphologies in BF_2^+ ion implanted (100) silicon

M. C. PAEK, H. B. IM
Department of Materials Science and Engineering, Korea Advanced Institute of Science and Technology, P.O. Box 131, Chongryang, Seoul, Korea

J. Y. LEE
Department of Materials Science and Engineering, Korea Institute of Technology, Daejeon, Korea

The effects of annealing on the damage morphologies and impurity redistributions in BF_2^+ ion implanted (100) silicon were studied using secondary ion mass spectrometry (SIMS), transmission electron microscopy (TEM) and Rutherford backscattering (RBS) ion beam channelling technique. An amorphized silicon layer and a heavily-damaged crystal layer containing a high density of point-defect clusters, are formed on the silicon wafer by the ion implantation. SIMS depth profiles of both boron and fluorine are almost Gaussian distribution. Both furnace annealing and rapid thermal annealing cause recrystallization of the amorphized layer and formation of dislocation loop bands out of the point defects. SIMS depth profiles for both impurities show anomalous double peaks at the same depths. These facts suggest that the primary peak is due to the peak of the Gaussian distribution and the secondary peak due to the gettering effects of residual dislocation loop band.

1. Introduction

Recently, the scale down trend of very large scale integration VLSI devices have required smaller dimensions both in lateral and vertical directions [1]. Memory devices with p^+/n junctions should have shallow junction depths and high acceptor concentrations to prevent electrical problems such as short channel and punch through effects [2, 3]. Ion implantation techniques have been used successfully for these requirements with high controllability of ion energy and dose. For n^+/p shallow junctions, As^+ ion implantation process can be adopted without serious processing problems. However, for p^+/n shallow junctions, conventionally used B^+ ion implantation process has some problems, caused by the relatively smaller mass of boron to silicon, such as deep projection range of boron, high channelling effect, and high density of crystal defects which consequently increase the reverse bias leakage currents.

BF_2^+ ion, co-produced with B^+ ion from BF_3 source gas in an ionization chamber, has (49/11) times higher mass than B^+ ion and higher ion beam currents. Therefore, the projection range of boron in BF_2^+ implantation is much shallower and the concentration can be higher than in B^+ implantation. Additionally, the amount of damages formed in silicon surface is much higher in BF_2^+ implantation, due to heavier mass and lower channelling effects, so the silicon can be easily amorphized during thermal annealing process by solid phase epitaxy.

For mega-bit complementary metal oxide semiconductors CMOS applications, the p^+/n junction depth should be less than 0.3 μm and sheet resistance lower than $100\,\Omega^{-1}$. To satisfy these requirements by BF_2^+ implantation, the energy and dose should be about 50 keV and $3 \times 10^{15}\,cm^{-2}$, respectively, and be annealed in lower temperatures or short periods to prevent deep diffusion of boron into depth [4, 5]. These processing conditions inevitably produce residual defects in electrically active regions during thermal annealing, and the mechanism and the thermal behaviours of the defects must be carefully understood to control the process.

In this paper, we present the results of a detailed investigation of damage morphologies produced by BF_2^+ ion implantation and by subsequent thermal anneal. The damage morphologies were examined by X-ray diffraction (XRD) patterns, cross-section transmission electron microscopy, and Rutherford backscattering ion beam channelling techniques. The effects of the damage defects on boron and flourine redistribution during the annealing were also investigated to study the electronic effects of these defects by taking the impurity depth profiles by SIMS.

2. Experimental procedure

(100) silicon wafers of 12.5 cm diameter and $5–10\,\Omega\,cm^{-1}$ resistivity were used. Silicon oxide of thickness 20 nm was thermally grown on the silicon

0022–2461/91 $03.00 + .12

surface at 950 °C in dry O_2, and BF^+ ions were implanted on the silicon substrate with 50 keV. The doses of the BF_2^+ ions used were 1×10^{15}, 5×10^{15} and 1×10^{16} cm^{-2}. Implanted specimens were annealed in the tube furnace at 950 °C for 40 min or rapid thermally annealed at 1150 °C for 15 s in dry N_2 ambient. These annealing conditions are reported to be sufficient to activate almost all boron ions.

With a secondary ion mass spectrometer, CAMECA ims-4f, the analysis has been carried out under positive oxygen ions (O_2^+) bombardment and positive secondary ions. Si^+ ions have been analysed as the reference signal of the matrix. Boron and fluorine have been analysed secondary intensities for $^{11}B^+$ and $^{19}F^+$ ions, respectively.

For cross-section transmission electron microscopy, thin-foil specimens were prepared by forming a sandwich with epoxy, followed by mechanical grinding and polishing to 20–50 μm thickness. Then they were attached to Cu made 3 mm one-hole grid, and argon ion milled in a specimen stage, cooled by liquid nitrogen to minimize ion milling damages. Fig. 1 shows the schematic diagram of the thin foil preparation sequence. In cross-section transmission electron microscopy, axial lattice images were taken in a [1 1 0] zone axis orientation wtih an objective aperture, which contained nine beams, on a Jeol jem-2000EX microscope equipped with a pointed LaB_6 filament and operating at 200 kV. Crystalline defects were characterized by diffraction contrast and specimen tilting. In Rutherford backscattering ion beam channelling techniques, a 2.275 MeV α-particle ($^4He^{2+}$) beam was accelerated in a pelletron-type accelerator and probed to [1 1 0] channelling direction. The backscattered α-particles were detected by Si surface barrier detector at a grazing angle of 110°.

3. Results and discussion

3.1. Secondary ion mass spectrometry

SIMS technique has been useful for the depth profile of several impurities with high detection limit, simultaneously. Fig. 2 shows the depth profiles of boron and fluorine from SiO_2 surface to the depth in silicon for the specimens, BF_2^+ implanted with 50 keV energy and dose of 5×10^{15} cm^{-2}, before and after thermal annealing. Before annealing, both impurities show almost Gaussian distribution which is well known distribution in ion implanted specimens. The peak concentrations of boron and fluorine are 8×10^{20} cm^{-3} and 1.3×10^{21} cm^{-3}, respectively. The projection ranges, the depths at which the concentration peaks occur, for both boron and fluorine were measured to be 38 nm in SIMS profiles, and considering the 20 nm thickness of oxide, the depths of the concentration peak in silicon were approximately 18 nm. After furnace annealing at 950 °C for 40 min,

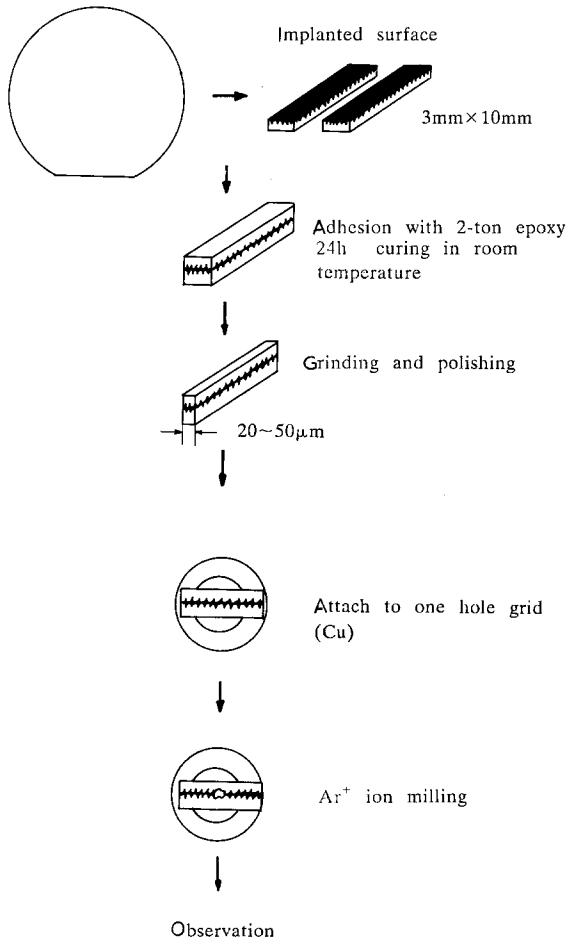

Figure 1 Thin section preparation sequence for cross-section observation of the implanted damages with transmission electron microscope.

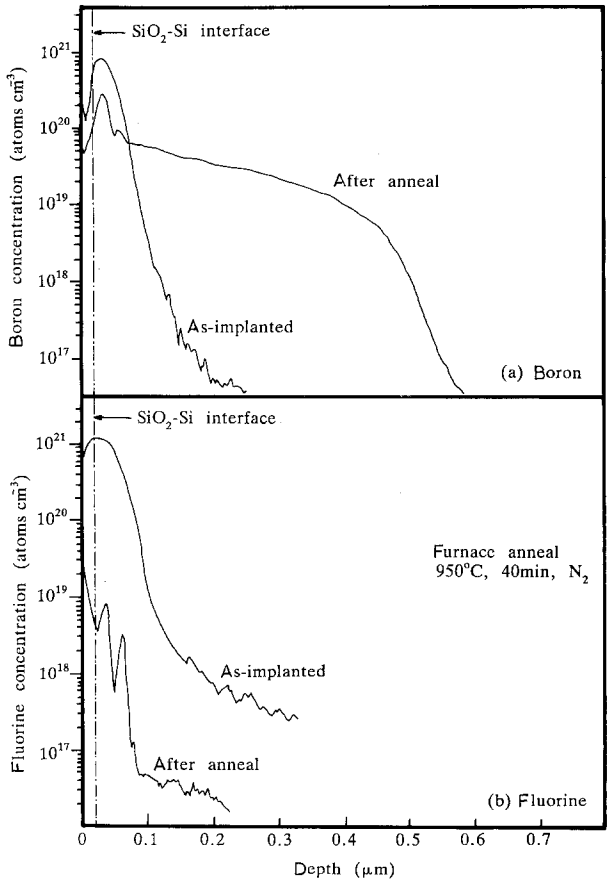

Figure 2 SIMS concentration depth profiles of (a) boron and (b) fluorine in BF_2^+ ion implanted (1 0 0) silicon by 50 keV energy and 5×10^5 cm^{-2} dose for as-implanted and after annealing for 40 min at 950 °C.

the depth profile for boron (Fig. 2a) shows an anomalous double peak which is similar to the one that reported by Lunnon and Chen [6]. It is interesting to note, however, that not only do the double peaks occur in the depth profiles for fluorine as well but also the second peak is much clearer (Fig. 2b). The depths at which the peaks occur are identical for boron and fluorine and are approximately 38 nm and 70 nm from the surface. The fact that the depths of the double peaks are independent of type of impurity suggests that the anomalous peak formation is caused by properties of defects generated by BF_2^+ ion implantation rather than by the properties of the impurity itself. It is reported that the implanted BF_2^+ ion decomposes into boron and fluorine ions in silicon. The fluorine ions, with higher diffusivity and lower solubility in silicon than in boron, diffuse a longer distance and out-diffuse from the surface and consequently the overall concentration of fluorine in the annealed specimen becomes lower than that of boron by two orders of magnitude. Fig. 2b also shows a high concentration of fluorine in the SiO_2 surface. The solubility of fluorine in SiO_2 is not reported but the value may be higher than that in silicon. To clarify this phenomena, BF_2^+ ions were implanted on (1 0 0) silicon without a SiO_2 layer.

Fig. 3 shows SIMS depth profiles of boron and fluorine before and after rapid thermal anneal at 1150 °C for 15 s for the specimens implanted with 1×10^{15} cm^{-2} dose onto bare silicon without capping oxide. The as-implanted profiles of both impurities show identical shape as in Fig. 2. However, the occurrence of the double peaks in the boron depth profile (a) can be seen more clearly. Again the depths at which the double peaks occur for boron and fluorine are identical, and are at 38 nm for the first peak and 65 nm for the second peak. The concentration of fluorine at surface after the anneal is much lower than that in Fig. 2b due to the absence of SiO_2 capping oxide.

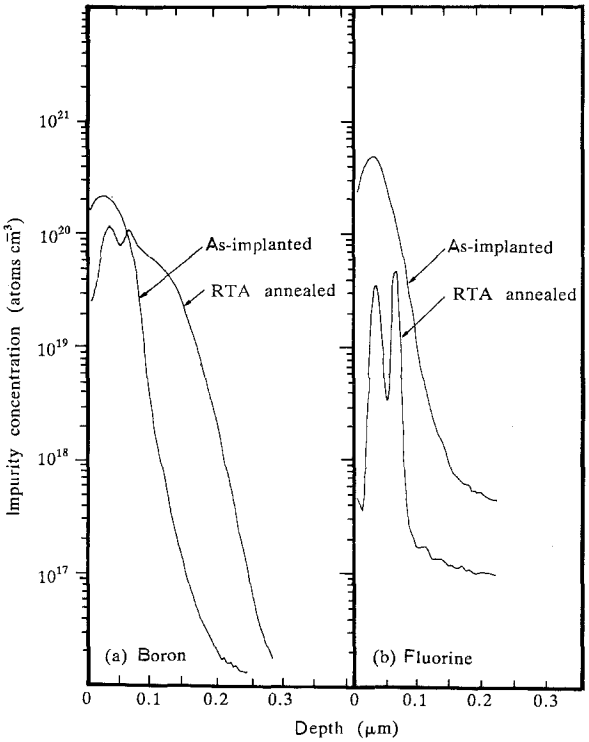

Figure 3 SIMS concentration depth profiles of (a) boron and (b) fluorine in BF_2^+ ion implanted by 50 keV energy and 1×10^{15} cm^{-2} dose showing double peaks in both impurities after rapid thermal annealing at 1150 °C for 15 s.

3.2. Transmission electron microscopy

A cross-section transmission electron microscopy image of an as-implanted specimen implanted by BF_2^+ ions with 50 keV energy and 1×10^{16} cm^{-2} dose is shown in Fig. 4. It shows a multi-layered structure of silicon substrate, amorphized silicon layer and capping oxide layer. The interface between amorphous and crystalline silicon show high contrast, and that between amorphous silicon and silicon oxide show relatively weak contrast. Because both silicon oxide and amorphous silicon have no crystallinity, the boundary between them is, in general, not clear. But by the difference of the density and thickness normal to the electron beam, which depends on the milling rate in ion milling step, the layers can be distinguished in the present specimen. The thicknesses of SiO_2 layer and amorphized silicon layer are approximately 20 nm and 60 nm, respectively. Fig. 5 shows the high resolution image of the layered structure, which has been taken of a very thin area of specimen. In the crystalline region, lattice lines are observed and the amorphous–crystalline interface is clearly shown with undulations of 2–5 nm amplitude. The random direction of recoiled and backscattered silicon ions, and the formation of point defect clusters are thought to be the main reasons for the undulation of the interface.

A high resolution electron micrograph of the amorphous–crystalline interface is shown in Fig. 6. In the crystalline layer near the crystalline–amorphous interface, micro-amorphous regions are observed

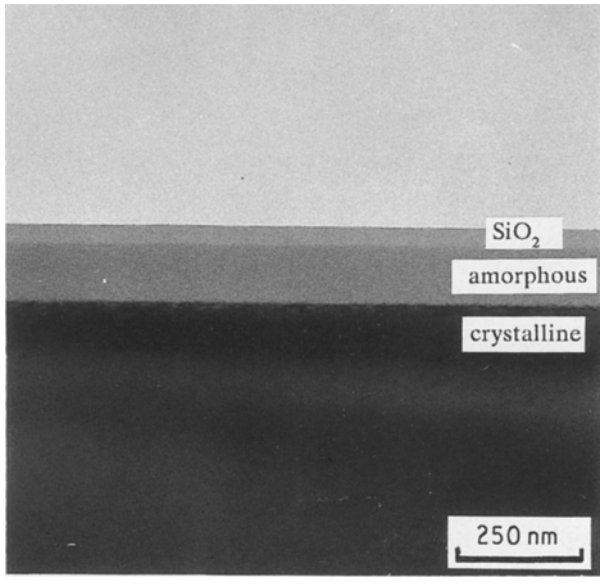

Figure 4 Cross-section transmission electron micrograph of as-implanted (1 0 0) silicon specimen (BF_2^+, 1×10^{16} cm^{-2}, 50 keV) showing layered structure of SiO_2, amorphous silicon and crystalline silicon substrate.

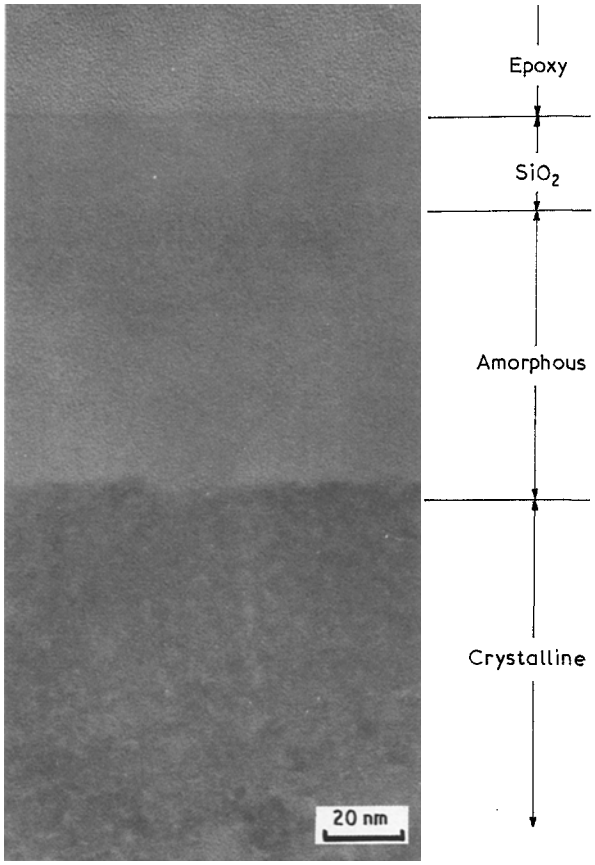

Figure 5 High resolution transmission electron micrograph of the layered structure.

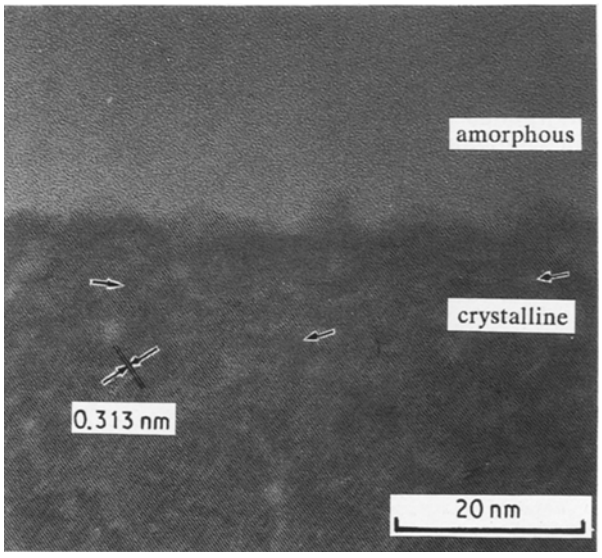

Figure 6 High resolution transmission electron micrograph of the amorphous–crystalline interface of Fig. 4 showing lattice distortions due to point defect clusters in crystalline silicon (arrow marks).

(indicated by arrow marks). It appears that the microscopic amorphous regions were formed by the accumulation of point defect clusters produced by BF_2^+ ion implantation. Looking along the lattice lines, it can be seen that the lines are distorted or disappear at these regions. The distance between the lines which corresponds to (1 1 1) layer spacing in silicon is 0.313 nm and is indicated in the figure. The angle between the (1 1 1) and (1 0 0) of the silicon substrate is 54.7°. The size of the micro-amorphous regions are about 2–5 nm in diameter. Some agglomerates and disc type defect clusters are also observed in lattice images. It is suggested that with high dose implantations, the crystalline layer changes to the amorphous state by nucleation and growth of the micro-amorphous region. Carter *et al.* reported on the critical size of embryo of these micro-amorphous regions [7]. Micro-amorphous regions were also observed in as-implanted specimen that was BF_2^+ ion implanted with 50 keV and 5×10^{15} cm^{-2} dose.

A cross-section electron micrograph of a specimen that was ion implanted with dose of 5×10^{15} cm^{-2} and was furnace annealed at 950 °C for 40 min is shown in Fig. 7. It can easily be seen that rather large spots exist parallel to surface in the crystallized silicon.

An enlarged cross-section microscope of the specimen of Fig. 7 is shown in Fig. 8 by diffraction contrast. To identify the nature of this defect, the diffraction contrast experiment with tilting about the (1 1 0) axis was carried out. It has been found that the defect spots consist of dislocation loops. The depth of dislocation loop bands is about the same as the damaged crystalline region in as-implanted specimen. Below these defects, any crystalline defect cannot be observed. The area which had been amorphized by implantation changed to clean crystalline state without any observable crystal defect. Thus, it is suggested that the lattice damages produced in crystalline silicon by BF_2^+ ion implantation are changed to dislocation loops, which have a relatively stable structure, and distribute in a constant depth from the surface during annealing process of 950 °C for 40 min.

With the transmission electron microscopy, it was found that the recovery and recrystallization kinetics of amorphized and much damaged silicon layers are different.

3.3. RBS ion beam channelling spectra

To analyse the amount of damage in silicon generated by ion implantation and annealing process, the He^{2+} ion beam channelling technique was employed with 2.275 MeV incident energy. Fig. 9 shows random and

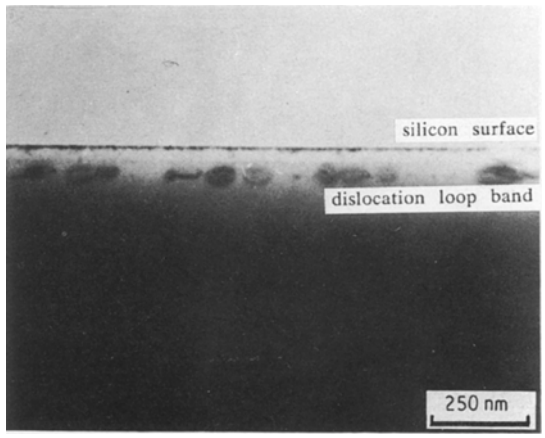

Figure 7 Cross-section electron micrograph of a specimen BF_2^+ ion implanted with dose of 5×10^{15} cm^{-2} and furnace annealed at 950 °C for 40 min.

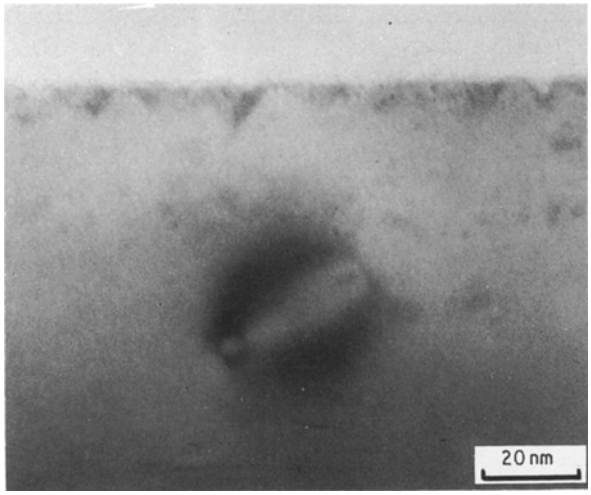

Figure 8 Enlarged image of a spot of Fig. 7.

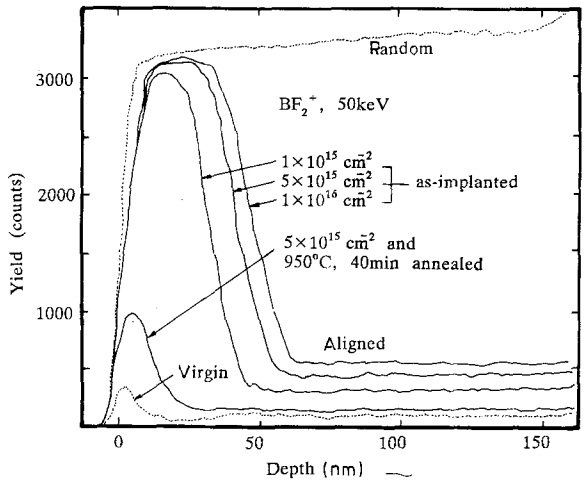

Figure 9 Rutherford backscattering ion beam channelling spectra of BF_2^+ implanted silicon at various stages.

aligned spectra of the specimens implanted by various doses and virgin crystal. In aligned spectra, we can see that the values of the backscattered yield in the top surface layer (20–30 nm deep) of as-implanted specimen reach that of the random spectrum, which means that the surface of the as-implanted specimens are fully amorphized. The broadening of the peak widths with increasing implant dose shows that the amorphization continues and the interface moves down as the implant dose increases. The thickness of the amorphous layers in as-implanted specimen increases with increasing dose of ion implantation, and the thicknesses are approximately 30 and 60 nm for ion dose of 1×10^{15} cm^{-2} and 1×10^{16} cm^{-2}, respectively. These values were consistent with the values determined from transmission electron micrographs. The aligned spectrum of after-anneal (950 °C, 40 min) show a much reduced yield of backscattering due to recovery and recrystallization processes. But, at the surface, a little backscattering yield is detected, which indicates that some interstitial type defects are still present in the region, although they were not observed by transmission electron microscopy.

4. Conclusions

Based on the results of analysis of cross-section transmission electron microscopy, Rutherford backscattering ion beam channelling technique and impurity depth profiles taken by secondary ion mass spectrometry of the BF_2^+ ion implanted (1 0 0) silicon before and after thermal annealing, the following conclusions can be drawn:

1. BF_2^+ ion implantations with energy of 50 keV and doses ranging from 1×10^{15} to 1×10^{16} cm^{-2} cause the formation of an amorphized layer and a heavily damaged crystalline layer with a high density of point defect clusters.

2. Furnace annealing for 40 min at 950 °C or rapid thermal annealing for 15 s at 1150 °C results in the recrystallization of the amorphised layer and the formation of dislocation loop bands out of the point defect clusters in the heavily damaged layer.

3. Both the boron and fluorine depth profiles show anomalous double peaks indicating that the formation of the peaks is independent of the type of impurity atoms.

4. These results suggest that the secondary peaks are caused by the gettering effect of the residual dislocation loop bands.

References

1. T. OHZONE, H. SHIMURA, K. TSUJI and T. HIRAO, *IEEE Electron Devices*, **ED-27** (1980) 1789.
2. I. W. WU, R. T. FULKS and J. C. MIKKELSON Jr., *J. Appl. Phys.* **60** (1986) 2422.
3. S. S. COHEN, J. F. NORTON and E. F. KOCH, *ibid.* **57** (1985) 1200.
4. M. E. LUNON and L. J. CHEN, *J. Electrochem. Soc.* **132** (1985) 2473.
5. Y. D. KIM and R. B. FAIR, *J. Elect. Mater.* **18** (1989) 143.
6. M. E. LUNNON and L. J. CHEN, *J. Appl. Phys.* **45** (1984) 1056.
7. C. CARTER, W. MASZARA, D. K. SADANA, G. A. ROZGONYI, J. LIU and J. WORTMAN, *Appl. Phys. Lett.* **44** (1984) 107.

Received 18 November 1989
and accepted 6 June 1990